Local structural order in nanostructured hematite

J. M. Florez · J. Mazo-Zuluaga · J. Restrepo

Abstract Nanostructured α-Fe$_2$O$_3$ powders were prepared by high-energy ball milling. The milling process spans grinding times from 30 min to 24 h. The as-milled samples were characterized by means of ^{57}Fe Mössbauer spectrometry, Rietveld analysis of X-ray diffraction data and particle size analysis. The obtained results evidence the presence of disordered hematite characterized by a hyperfine field distribution with a well-behaved dependence on the mean crystallite size for which the mean hyperfine field decreases asymptotically as the grain size decreases. A new relationship is proposed in order to describe such behavior. Finally the presence of superparamagnetic grains, the occurrence of a partial topotactic phase transformation into a spinel phase and tool induced contamination are also presented and discussed.

Key words Mössbauer · hematite · Rietveld · ball milling · nanostructure

1 Introduction

During the last decade, great attention has been paid to the magnetic and structural properties of nanostructured alloys [1], fluorides [2] and some iron oxides [3] for which a wide variety of grain boundary effects takes place. However a wider and deeper insight on the structural and magnetic properties of some nanostructured iron oxides like hematite is still remaining. These features are important to understand some mechanisms like those involved in the Morin transition [4–7]. In this work we stress on nanostructured hematite powders obtained through a vacuum grinding route for different milling times in a planetary ball mill. Their structural, microstructural and magnetic properties are investigated by

J. M. Florez · J. Mazo-Zuluaga · J. Restrepo (✉)
Grupo de Estado Sólido, Instituto de Física, Universidad de Antioquia, A.A. 1226 Medellín, Colombia
e-mail: jrestre@fisica.udea.edu.co

J. Mazo-Zuluaga · J. Restrepo
Grupo de Instrumentación Científica y Microelectrónica, Instituto de Física,
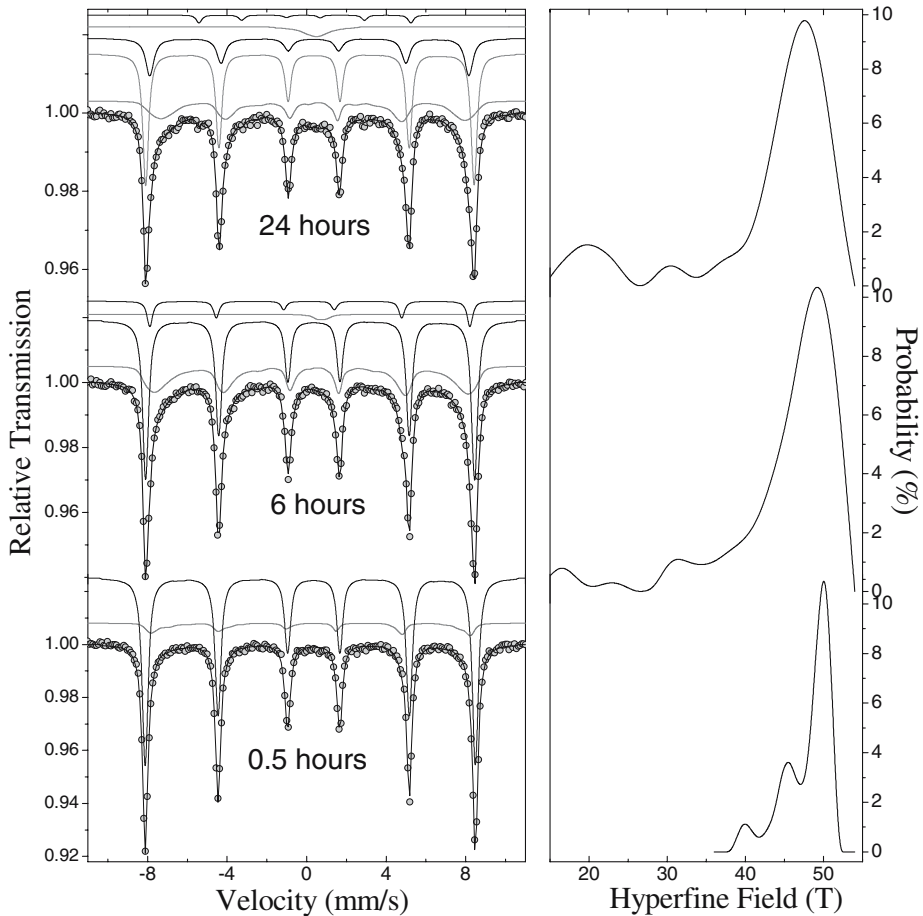Universidad de Antioquia, A.A. 1226 Medellín, Colombia

Figure 1 Room temperature Mössbauer spectra for 0.5, 6 and 24 h of milling and their respective hyperfine field distributions. The decomposition into components is shown.

means of transmission ^{57}Fe Mössbauer spectrometry at room temperature, Rietveld analysis of X-ray diffraction patterns and particle size analysis by laser scattering.

2 Experimental

Mechanical milling of 99.9% pure hematite (Merck) powders, with an average particle size of 4 μm, was carried out in a planetary ball mill Fritsch-Pulverisette5 by using Chromium-based stainless steel jars of 250 ml with balls of the same material and a diameter of 13 mm. The employed vessels were previously evacuated at 0.1 atm. Milling times of 0.5, 1, 3, 6, 12, 15, 18 and 24 h were considered using an average sample-balls weight ratio of 1:10. Every sample for every milling time was prepared separately in order to preserve the sample to balls weight ratio and to guarantee the absence of statistical correlation among them. Every sample was milled at 390 rpm for intervals of 1 h and break periods of 30 min up to complete the desired milling time. At the end of every milling interval both the

Table I Hyperfine parameters of the distributed component for the first milling stages

Milling time (h)	$2 e_Q$ (mm/s)	δ (mm/s)	B_{hf} (T)
0.5	0.010	0.671–0.059	36–54
1	−0.079	0.431–0.258	15–54
3	−0.138	0.508–0.243	15–54
6	−0.154	0.550–0.277	15–54

pressure and temperature were monitored. This last one ranged between 35 and 41°C. The obtained as-milled samples were analyzed by means of ^{57}Fe Mössbauer transmission spectrometry at 296 K, X-ray diffraction and laser scattering for particle size analysis. Mössbauer spectra were fitted using the Normos-Distri program [8]. All fittings involved the presence of at least one hyperfine field distribution (HFD) according to the observed line broadenings. Isomers shifts are quoted relative to α-Fe. X-ray diffraction analysis was performed using a Bruker AXS Advance D8 diffractometer with Co tube and Fe filter in the 2θ range of 20–70° every 0.014° and 4 s per step. Diffraction patterns were fitted using the MAUD program (http://www.ing.unitn.it/~luttero/maud/) based on the Rietveld method from which phase distribution, cell parameters, mean crystallite size, microstrain and volume fractions were obtained.

3 Results and discussion

Figure 1 shows the Mössbauer spectra for three selected milling times. In addition to the HFD, a well defined crystalline component accounting for the observed kinks in the external absorption lines was also considered. The fitted hyperfine parameters of this last component are B_{hf}=51.4(3) T, $2\varepsilon_Q$=−0.20(1) mm/s and δ=0.38(1) mm/s, which clearly correspond to the precursor hematite. The corresponding relative area of this component decreases as milling time increases. Concomitantly, the spectral area of the distributed component increases and the HFD becomes progressively broader in agreement with a higher degree of disorder. Table I shows the hyperfine parameters of the distributed component for the first milling stages whereas the milling time dependence of the relative areas is shown in Figure 2. Figure 3 shows some selected diffractograms including Rietveld fitting. In all cases two hematite components were employed: One of them preserving structural parameters of the precursor hematite. The second one was fitted revealing a progressive volume fraction increase and a marked reduction of the mean crystallite size in correspondence with the HFD via Mössbauer. Several features are particularly interesting like the fractional variations of the lattice parameters a and c of the free hematite component as shown in Figure 4. The observed behavior reveals a mechanical dilation anisotropy where the unit cell volume tends to be more easily deformed along the basal plane instead of the c axis. In fact, the average unit cell volume expansion was as higher as 0.5%. We think the observed deformation anisotropy should play a key role as a magnetovolume effect in the explanation of the Morin transition, since as is established the spin canting observed in hematite involves a preference of the spins to lie along the basal plane [9]. Such a degree of deformation agrees with the observed variation of the root mean square microstrain ranging from 0.0049 up to 0.011 and becoming stable at around this last value beyond 3 h of milling. On the basis of these results and in order to elucidate the influence of the structural parameters upon the hyperfine ones we have carried out several correlations including the dependence of the mean hyperfine field on both the unit cell average volume of hematite and the mean crystallite size. In the former, the mean

Figure 2 Milling time dependence of the increasing relative areas obtained via Mössbauer. The different employed components are exhibited. Label *SP* stands for superparamagnetic grains. *Lines* are guides to the eye.
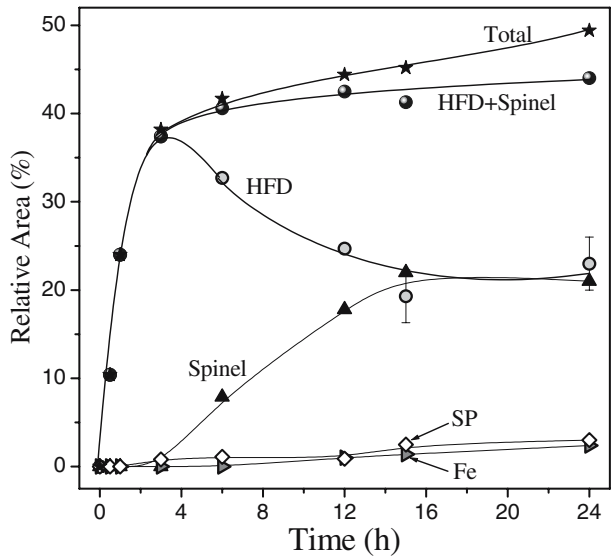
hyperfine field decreases smoothly with the unit cell volume up to around 909 Å^3 where $\langle B_{hf} \rangle$ exhibits a sharp decrease down to almost 40 T. Such reduction corresponds to 21% relative to the hyperfine field of pure hematite. This remarkable decrease is ascribed to the milling-driven increase of the nearest neighbor distance for which the dipolar contribution to the magnetic hyperfine field becomes smaller. The correlation of $\langle B_{hf} \rangle$ with the mean crystallite size is shown in Figure 5 which can be fitted by the following proposed relationship:

$$\langle B_{hf} \rangle = B_0 - \frac{\alpha}{\langle D \rangle + (\alpha/B_0)}, \tag{1}$$

where $\langle D \rangle$ accounts for the mean crystallite size, B_0 is the hyperfine field of the precursor hematite and α is a fitting parameter ruling out the way as the mean hyperfine field goes to zero as the mean crystallite size decreases. This expression complements that proposed by Murad and Schwertmann [10], and it describes better the behavior of the mean hyperfine field in those limit cases where the mean crystallite size goes to infinity (an extended and homogeneous single-crystalline hematite) or when it goes to zero, for which $\langle B_{hf} \rangle$ vanishes, corresponding to the superparamagnetic limit. Such decrease is attributed to a milling-induced higher degree of disorder. Moreover, the decrease of the mean hyperfine field must be linked to those grain boundaries and interfacial regions where the degree of disorder is greater. In correspondence, the employed hematite crystalline component can be attributed to the core of the grains with a progressive decrease of the relative area as we have already mentioned.

On the other hand, as milling time goes beyond 3 h, a doublet (Γ=0.9 mm/s, δ= 0.55 mm/s, ΔE_Q=0.31 mm/s) is necessary to get a good fit of the central region in Mössbauer spectra (see Figure 1). Such a signal is attributed to the occurrence of superparamagnetic grains having sizes smaller than 8 nm for which a superparamagnetic relaxation is expected [12]. The presence of those grains is endorsed by the obtained grain size distribution centered at around 11 nm in agreement with that fraction of hematite corresponding to the distributed component, i.e. grain boundaries and interfacial regions.

Figure 3 X-ray diffractograms, including Rietveld fitting for the precursor material, 0.5, 3 and 12 h of milling. Two hematite components were employed, one of them for the core of the grains and the other one accounting for grain boundaries and interfacial regions.
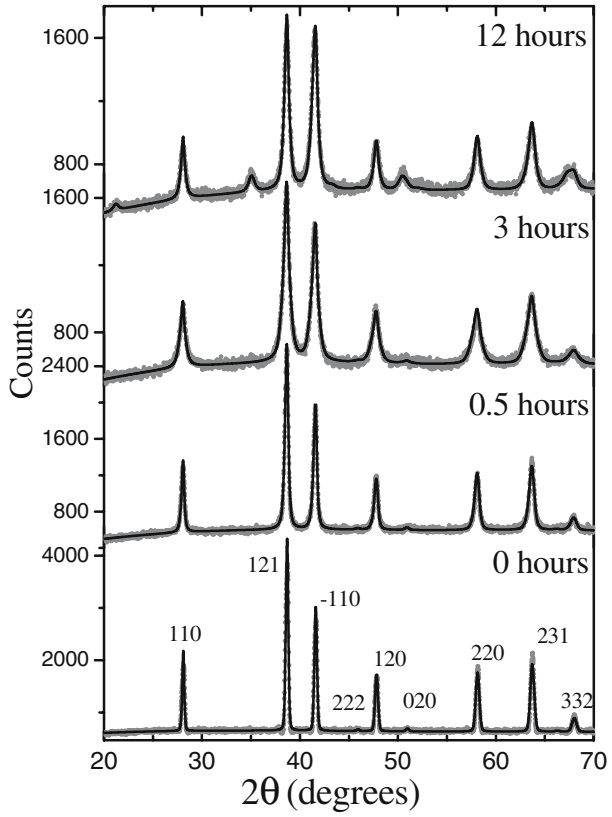

Figure 4 Fractional variations of the lattice parameters a and c for the distributed hematite component obtained via Mössbauer. *Lines* are guides to the eye.
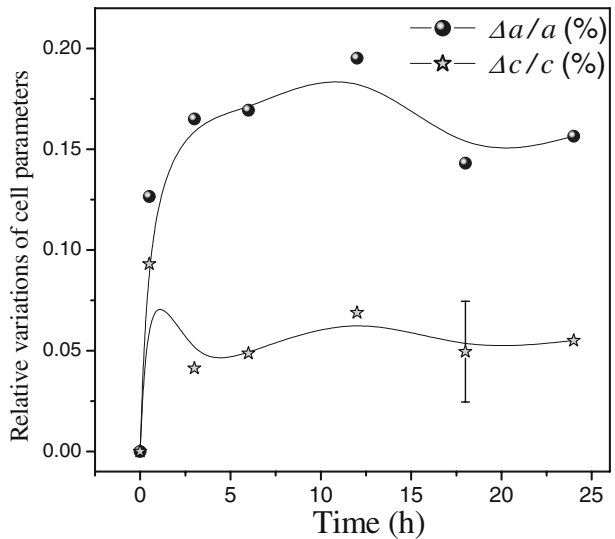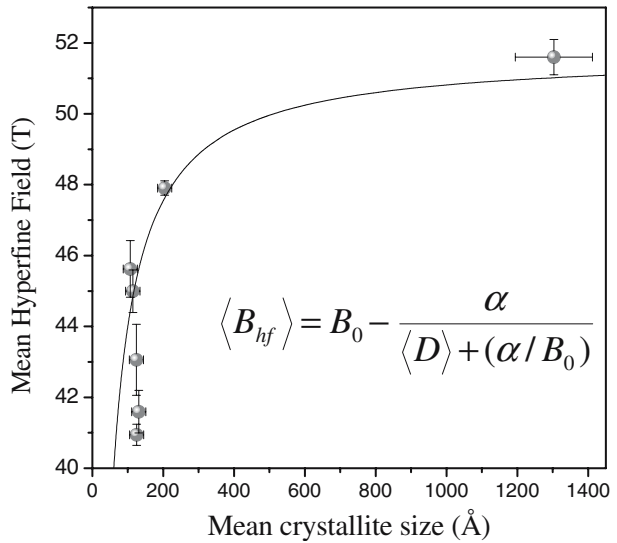
Figure 5 Mean crystallite size dependence of the mean hyperfine field $\langle B_{hf} \rangle$. Inset shows the fitting relationship describing the observed behavior, where B_0 corresponds to the hyperfine field of pure hematite (51.6 T) and $\langle D \rangle$ in Å accounts for the mean crystallite size. The parameter α giving the best fit was 900 TÅ.

$$\left\langle B_{hf} \right\rangle = B_0 - \frac{\alpha}{\langle D \rangle + (\alpha / B_0)}$$

For milling times above 6 h, an additional component must be included in the fitting process corresponding to a spinel phase having B_{hf}=49.8 T, $2\varepsilon_Q$=−0.08 mm/s, and δ= 0.30 mm/s, which could be ascribed to a maghemite phase [10]. The relative area of this component is also shown in Figure 2. The onset of this component is endorsed by X-ray diffraction data for which two new Bragg peaks become evident at 35.0 and 50.6° and can easily be indexed by Rietveld analysis to a magnetite or maghemite phase. However, since magnetite involves the presence of Fe^{2+} ions in octahedral crystallographic sites, for which a reduction from hematite is needed, it makes more sense to assign this new phase to maghemite, which involves only Fe^{3+} like in the precursor material, preserving the molecular formula. From this point of view, this spinel component can therefore be ascribed to a topotactic isochemical transformation from hematite due to the imparted energy during the milling process. For milling times above 12 h a sextet corresponding to α-iron was detected with relative area below 2.5%. The presence of this phase, which is also observable through diffractograms, is attributed to contamination arising from milling tools [13]. Finally, measurements on particle size through laser scattering, evidenced particle sizes in the range 0.1–500 μm endorsing a scenario of micrometric nanostructured particles.

4 Conclusions

The obtained results reveal a partial transformation (less than 23%) of the precursor hematite into a spinel phase attributed to maghemite. However, despite the presence of this spinel phase, the employed milling conditions delays the complete transformation of hematite contrary to what has been found in wet milling conditions by using the same type of mill [14]. The observed doublets in Mössbauer spectra (less than 2.5%), for milling times above 3 h, are attributed to superparamagnetic grains. On the other hand, a worthy relationship between the mean crystallite size and the mean hyperfine field of the distributed hematite component has been proposed through the correlation between Mössbauer results and Rietveld analysis. Our results endorse some of the findings reported

by Stewart et al. [5] and Bruzzone and Ingalls [15] related to the effect of milling-induced disorder and the effect of pressure upon the magnetic properties of hematite.

Finally, the observed results allow proposing a scenario of nanometric crystalline grains with interfacial regions characterized by a high degree of atomic disorder. Such a state is ruled out by an anisotropic mechanical dilation for which a higher fractional variation of the *a* parameter was observed. Correspondingly the mean hyperfine field decreases with the progressive evolution of this state as the milling time increases.

References

1. Miglierini, M., Greneche, J.M., Idzikowski B.: Mater. Sci. Eng. **A304-306**, 937 (2001)
2. Guérault, H., Bureau, B., Silly, G., Buzaré, J.Y., Greneche J.M.: J. Non-Crryst Solids **287**, 65 (2001)
3. Randrianantoandro, N, Mercier, A.M., Hervieu, M., Greneche, J.M.: Mater. Lett. **47**, 150 (2001)
4. Kletetschka, Günther, Wasilewski, Peter J.: Phys. Earth Planet. Inter. **129**, 173 (2002)
5. Stewart, S.J., Borzi, R.A., Cabanillas, E.D., Punte, G., Mercader, R.C.: J. Magn. Magn. Mater. **260**, 447 (2003)
6. Amin, N. Arajs, Sigurds: Phys. Rev., B. **35**, 4810 (1987)
7. Zysler, R.D., Fiorani, D., Testa, A.M., Suber, L., Agostinelli, E., Godinho, M.: Phys. Rev., B. **68**, 212408–212411 (2003)
8. Brand, R.A.: Nucl. Instrum. Methods Phys. Res., B. **28**, 417 (1987)
9. Dang, M.Z., Rancourt, D.G., Dutrizac, J.E., Lamarche, G., Provencher, R.: Hyperfine Interact. **117**, 217 (1998)
10. Murad, E., Schwertmann, U.: Clays Clay Miner. **34**, 1 (1986)
11. Cornell R.M., Schwertmann U.: The Iron Oxides. VCH, Weinheim (1996)
12. Rancourt, D.G., Julian, S.R., Daniels, J.M.: J. Magn. Magn. Mater. **49**, 305 (1985)
13. Sánchez, F.H., Rodríguez Torres, C.E., Fernández van Raap, M.B., Mendoza Zélis, L.: Hyperfine Interact. **113**, 269 (1998)
14. Betancur, J.D., Restrepo, J., Palacio, C.A., Morales, A.L., Mazo-Zuluaga, J., Fernández, J.J., Pérez, O., Valderruten, J.F., Bohórquez, A.: Hyperfine Interact. **148/149**, 163 (2003)
15. Bruzzone, C.L., Ingalls, R.: Phys. Rev. B. **28**, 2430 (1983)